AGU PUBLICATIONS

Geophysical Research Letters

RESEARCH LETTER
10.1002/2016GL067697

Key Points:
- Supraglacial stream networks are controlled by bedrock topography, ice flow, and fluvial erosion
- Stream profiles indicate tendency toward topographic steady state
- Slope and concavity of equilibrium channel profiles are sensitive to ice flow regime and melt rate

Supporting Information:
- Supporting Information S1

Correspondence to:
L. Karlstrom,
leif@uoregon.edu

Citation:
Karlstrom, L., and K. Yang (2016), Fluvial supraglacial landscape evolution on the Greenland Ice Sheet, *Geophys. Res. Lett.*, *43*, doi:10.1002/2016GL067697.

Received 8 JAN 2016
Accepted 3 MAR 2016
Accepted article online 10 MAR 2016

Fluvial supraglacial landscape evolution on the Greenland Ice Sheet

Leif Karlstrom[1] and Kang Yang[2]

[1]Department of Geological Sciences, University of Oregon, Eugene, Oregon, USA, [2]Department of Geography, University of California, Los Angeles, California, USA

Abstract Supraglacial stream networks incise via thermal erosion of underlying ice, reflecting a balance between localized fluvial incision and dynamic topography from underlying ice flow. We analyze high-resolution digital elevation models of the ice surface and bedrock in the southwest Greenland Ice Sheet from 1000-1600 m elevation to quantify the importance of fluvial erosion. At wavelengths greater than ice thickness, bedrock dominates surface topography so supraglacial drainage basins are fixed spatially. At smaller wavelengths, fluvial erosion significantly affects topography. Stream longitudinal profiles exhibit positive mean curvature and consistent power law scaling between local channel slope and drainage area, suggestive of adjustment toward topographic steady state. We interpret these observations with a model for fluvial thermal erosion on top of a flowing ice substrate that predicts concave up steady state longitudinal profiles, where average concavity is most sensitive to melt rate and the relative magnitudes of ice flow and fluvial erosion.

1. Introduction

In the ablation zone of glaciers and ice sheets, melting during summer months results in development of supraglacial streams and lakes that route melt water downslope until it is sequestered by the englacial system or (less commonly) flows off the edge of the glacier [*Fountain and Walder*, 1998; *Smith et al.*, 2015]. This supraglacial drainage network sets the efficacy by which melt water is transport into the glacier and thus has important implications for coupling between glacier sliding and surface melt [e.g., *Müller and Iken*, 1973].

Supraglacial streams evolve via thermal erosion, incising more rapidly than surrounding ice due to the presence and flow of liquid water. Incision is strongly coupled to solar radiation leading to diurnal fluctuations in discharge [e.g., *Marston*, 1983]. Thermal erosion in supraglacial streams is rapid compared to other fluvial environments, with absolute daily incision up to $\sim$ 10 cm, and relative daily incision (with respect to the surrounding ice, which is also melting) of several centimeters [*Isenko and Mavlyudov*, 2002]. This seasonal contribution to glacier surface evolution results in the development of widespread fluvial channel networks across the ablation zone. Planform features associated with bedrock and alluvial channels are common, making the supraglacial fluvial system attractive as an analog to terrestrial landscape evolution [e.g., *Montgomery and Dietrich*, 1992], and fluvial channel networks on other planets [e.g., *Baker et al.*, 2015].

It is not known however to what extent supraglacial drainage evolution is driven by exogenic factors or whether local fluvial incision of stream channels is significant on the scale of closed drainage basins that cover the ablation zone. Exogenic drivers of stream evolution include underlying bedrock topography expressed at the surface, changes in the flow rate of underlying ice, and sudden base level changes such as due to drainage of supraglacial lakes into the englacial hydrologic system. Bedrock exerts persistent control on glacier surface topography over wavelengths similar to ice thickness [e.g., *Raymond and Gudmundsson*, 2009; *Lampkin and VanderBerg*, 2011]. Variations in ice flow from environmental perturbations [e.g., *Nye*, 1963] generate dynamic topography that both advects with the glacier and migrates relative to dominant flow [e.g., *van de Wal and Oerlemans*, 1995; *Gudmundsson et al.*, 1998]. Because summer surface lowering rates in the ablation zone are often comparable to or greater than typical ice flow rates [e.g., *McGrath et al.*, 2011], fluvial processes may also significantly modify the ice surface.

Here we explore this latter possibility by studying complete supraglacial drainage basins in four regions that form an elevation profile of southwest Greenland Ice Sheet (Figure 1). We use a combination of high-resolution satellite images and concurrent digital elevation models (DEMs) to asses the relative contributions of exogenic

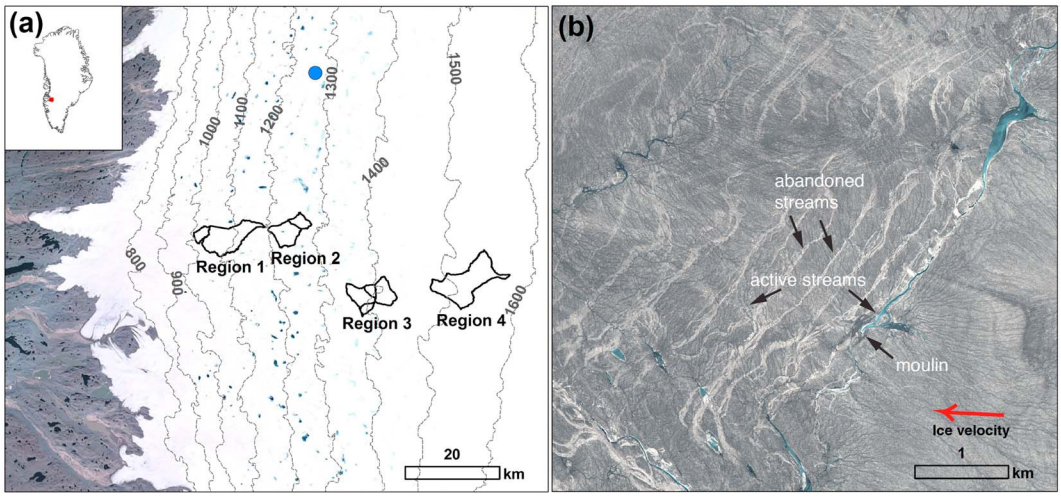

Figure 1. (a) Map and large-scale topography of study area in southwestern Greenland. Complete drainage basins are outlined. (b) World View imagery of the area denoted by the blue dot in Figure 1a, annotated to show abandoned streams advected downstream of active streams (which crosscut abandoned streams) and moulin. Red arrow is the average ice velocity over the image from MEaSUREs, with magnitude 49.2 ± 4.9 m/yr and direction 180.3 ± 8.2° from east.

and fluvial drivers of the supraglacial drainage system. DEMs aided by visual imagery are used to extract stream channel networks from surface topography and compare spectral characteristics with underlying bedrock topography.

We find that bedrock controls large-scale features of supraglacial stream networks, but roughness due to fluvial incision appears to dominate topography at 100 − 200 m wavelengths and shorter. Channels in this wavelength band commonly exhibit concave up distance-elevation (longitudinal) profiles, suggesting that stream topography evolves toward a steady state with the underlying flowing ice substrate. We develop a model for longitudinal profiles in supraglacial streams that integrates the effects of ice flow with solar driven melting and viscous dissipation of heat by flowing water. Parameter sensitivity tests demonstrate that average steady state profile concavity and slope are sensitive to local ice flow parameters as well as to the surface energy balance and are consistent with the range of these parameters found in our study area.

2. Methods

We use high-resolution ice surface DEMs [*Noh and Howat*, 2015] from the 2011 melt season to conduct a systematic survey of supraglacial channels, comparing with concurrent WorldView-1 (WV1) satellite imagery, bedrock topography, and ice surface velocity models (date information in supporting information). We choose a study area of four regions with increasing elevations in a trend roughly perpendicular to the ice sheet margin (Figure 1a), spanning most of the active ablation zone but avoiding near-marginal regions with high-crevasse density. While there is evidence for fractures and some structural control of drainages, much of our study area is crevasse free. The bedrock topography DEM is constructed from surface elevation and radar soundings with spatial resolution of 150 m [*Morlighem et al.*, 2013]. We compare two ice velocity models: the 2009 MEaSUREs model [*Joughin et al.*, 2010b] and the 2015 Sentinel-1 model [*Nagler et al.*, 2015]. Neither are concurrent with the surface DEMs, but average ice velocity magnitudes and directions for the study area are identical within error for both. We report only MEaSUREs values here as it is closest to the imagery date. Sentinel-1 values are reported in the supporting information Table 1.

Ice surface Stereo-Photogrammetric digital elevation models (spatial resolution 2 m) released by the Polar Geospatial Center and the Byrd Polar Research Center Glacier Dynamics Group (http://www.pgc.umn.edu/elevation/stereo) are used in this study. This DEM is constructed from overlapping pairs of WV1 panchromatic stereo images (0.5 m) acquired in a very short time interval (generally less than a minute). The reported root-mean-square error (RMSE) for this product is 3.8 m in the horizontal and 2.0 m in the vertical [*Noh and Howat*, 2015]. Fluvial drainage networks are easily extracted from high-resolution digital topography if these drainages have high enough interconnectivity and relief. However, in the supraglacial environment numerous small-scale topographic depressions exist on the ice surface that host supraglacial lakes or moulins,

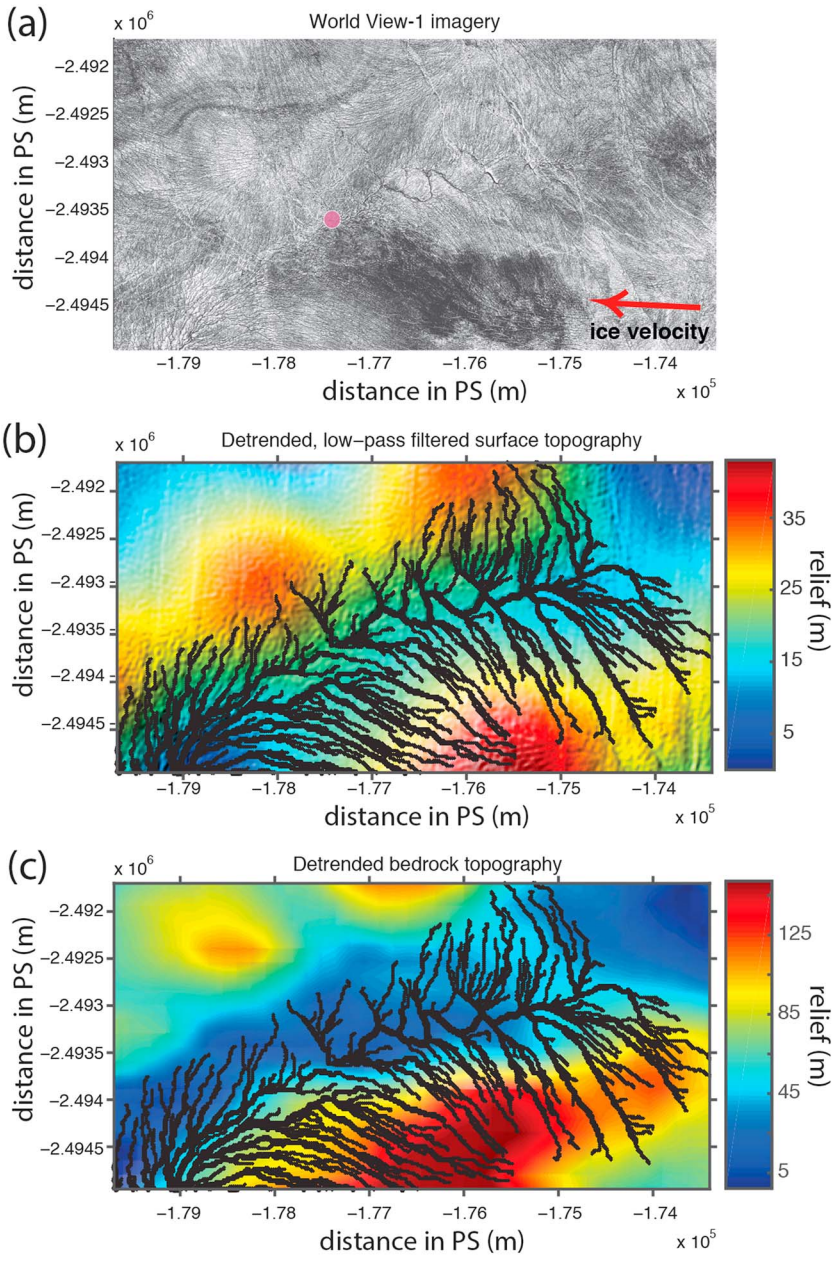

Figure 2. (a) World View imagery of a portion of Region 2 (acquired 30 August 2011), with moulin labeled by the pink dot and average velocity vector from MEaSUREs, with magnitude 98.8 ± 7.0 m/yr and direction 178.8 ± 2.6° from east. Projection is Polar Stereographic. (b) Hillshade image of detrended and low-pass filtered ice surface DEM. Channels overlaid with thicker lines have drainage areas larger than 10^5 m^2. (c) Hillshade of detrended bedrock DEM, with surface channels overlaid.

and the relief across a catchment is low (e.g., Figures 2a and 2b). These depressions act as meltwater sinks and fragment the supraglacial drainage networks but are not easy to distinguish from DEMs and therefore pose a problem for delineating supraglacial drainage networks using solely digital topography [*Yang et al.*, 2015]. To address this problem, contemporaneous WV1 panchromatic images are acquired from the DigitalGlobe Inc. through the Polar Geospatial Center. We use WV1 images as ground truth to identify meltwater sinks, which are subsequently prescribed as internal basin outlets to extract supraglacial drainage networks from WV1 DEMs. Our study area contains nine complete drainage basins (Figure 1a).

Even with the WV1 DEMs, small-scale channels (that can extend down to ~1 cm widths in some settings) [*Karlstrom et al.*, 2013] are likely below the resolution of imagery. The threshold minimum drainage area

chosen to create channel networks from WV1 DEMs (and hence the smallest channels) is 2×10^4 m^2. Resulting channel networks are somewhat sensitive to this threshold but we consider it an upper bound since, due to the low relief of channels compared to the vertical RMSE of 2 m, channel profiles with lengths $\leq 30-40$ m appear noisy. We extract hundreds of channels per region in Figure 1 above this threshold. To estimate local slope and upstream curvature from channels, we smooth raw profiles of channel centerline elevation. Channel and catchment statistics over the entire study area and per region are summarized in the supporting information; we use Region 2 to illustrate our results here.

We transform the DEM to the frequency domain using a discrete Fourier transform (DFT) and then spectrally filter to remove high frequency noise with a 2-D linear low-pass or band-pass filter. DFT spectral power density is visualized using radial frequencies to construct a 1-D spectrum [*Perron et al.*, 2008b].

3. Topography of Supraglacial Drainages and Glacier Surface Landscape Evolution

Glacier and ice sheet surface shape at the largest scales reflects a basic balance between gravitational forces and mass balance with ice deformation and sliding [*Cuffey and Paterson*, 2010]. At scales similar to ice thickness the topography of the bedrock underlying the ice mass sets surface topography (with some dependence on basal sliding). Wavelengths between 3 and 8 times the ice thickness are most effectively transferred from the bed to the surface [e.g., *Gudmundsson*, 2003; *Raymond and Gudmundsson*, 2009].

Supraglacial lakes have been found to correlate well with lows in bedrock topography and thus surface depressions are fixed spatially on yearly timescales [*Lampkin and VanderBerg*, 2011]. At shorter wavelengths roughness from surface features such as crevasses and water flow appear [*Rippin et al.*, 2015]. High-resolution images of the surface reveal abandoned channels advected downstream of apparently fixed large streams and lakes (Figures 1b and S3), with active streams cross cutting them. Spacing of abandoned channels in our study region is within a factor of ~2 average ice speeds [*Joughin et al.*, 2010a], a good match considering that not all persistent hydrologic features reform every year [*Liang et al.*, 2012].

Supraglacial drainage basins on the Greenland Ice Sheet range greatly in scale, with the longest streams (and thus drainage basins) yet found in the ~30 – 50 km range [*Poinar et al.*, 2015]. The drainage basins in our study area are slightly smaller (Figure 1), with maximum channel length per basin varying between 5 and 15 km. In our study area, ice thickness increases with elevation (as is generally the case) varying between ~900 and 1400 m. Maximum channel lengths are thus in a range where bedrock topography, if present, should affect ice surface topography. In our relatively small data set, maximum channel lengths covary with elevation but drainage areas do not, which could suggest exogenic control on catchment size rather than fluvial drainage organization.

Spectral analysis of detrended DEMs also supports this hypothesis: comparison of bedrock and surface spectra for each basin is very similar for wavelengths greater than ~1 km, with peaks in bedrock spectra mimicked by the surface. We illustrate this relation for Region 2 (Figure 3), but similar patterns occur in all our study regions (Figure S4). Amplitudes of bedrock topography are generally about an order of magnitude greater than surface undulations, and surface topography is often offset in space from bedrock peaks (Figure 2) consistent with pile ups caused by ice advection [*Raymond and Gudmundsson*, 2009].

Although the bedrock DEM does not resolve structures at wavelengths smaller than ~200 m, we see in all basins a new set of surface DEM spectral peaks between ~10 and 200 m wavelengths with a maximum around 20 – 30 m (Figure 3a). By band-pass filtering the DEM in this frequency band (Figure S5) it is clear that these peaks are due to supraglacial streams and crevasses (although crevasses are not a dominant surface feature in our study area). The broad peak in binned averages (black circles in Figure 3a) is consistent with active stream spacing, but nonactive streams may also contribute longer wavelength peaks at 50 – 200 m due to yearly advection of surface features at the local ice velocity.

Stream elevation-distance profiles also reflect a wavelength dependence of contributing processes. In a range of drainage areas from $\sim 10^5$ to 10^6 m^2 (some slight variation between regions), there is a power law decrease in local downstream slope with drainage area. The best fitting exponent for all regions in this range is $-5 \times 10^{-3} \pm 1.1 \times 10^{-3}$ (fitting binned averages within the gray shaded region of Figure 3b, supporting information Table 2). We also see positive longitudinal profile curvature in this range (Figure 3c), consistent with fluvial erosion and adjustment toward steady state topography [*Whipple and Tucker*, 1999]. At smaller drainage areas,

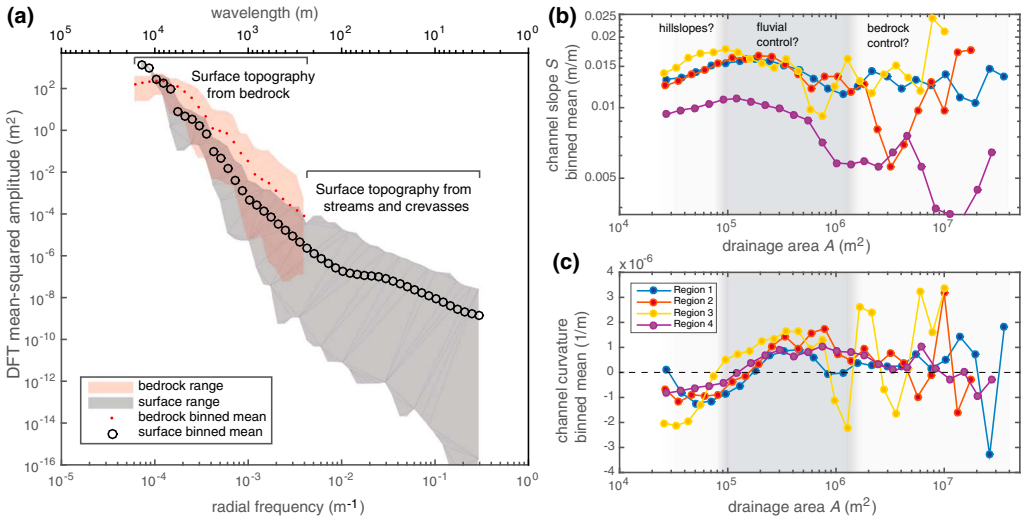

Figure 3. (a) One-dimensional power spectrum of detrended topography for Region 2, bedrock (red, shows maximum/minimum limits) and surface (gray) DEMs. Spectral slope and peaks in surface spectra broadly agree with bedrock at long wavelengths, with a slope break at 100–200 m that reflects surface features (streams and more rarely crevasses). (b) Mean local slope of stream channels smoothed from the raw DEM for each region. Shading indicates possible fluvial control, and a fit to binned averages in this range (at least 1000 samples per bin) gives $S = 0.04A^{-0.005}$ (supporting information). (c) Mean local curvature of stream channels for each region.

slope in all regions increases with area and channels are concave down, as would be expected from a diffusive process controlling topography [*Montgomery*, 2001]. We will suggest in the next section that diffusion from ice flow and melting generates this trend, although noise from the DEM small wavelengths may also contribute. At larger drainage areas, average slopes and curvatures are not similar between regions, as would be expected from variable bedrock topography.

Spectral and channel profile analysis thus supports a phenomenological model for supraglacial landscape evolution with two components. Yearly flow of ice into and out of bedrock depressions broadly determines the locations of supraglacial drainage basins which then dry out and advect downstream during the winter. Within these catchments, active fluvial erosion sculpts the landscape on smaller scales during the summer, creating low-relief valleys and channel networks that evolve over the course of the melt season.

4. Do Supraglacial Streams Achieve Erosional Equilibrium?

Bedrock rivers generally erode toward a steady state concave up along-stream elevation profiles for which erosion balances uplift at all points along the channel [*Gilbert*, 1877]. While supraglacial streams actively erode their substrate and there is dynamic topography due to ice flow, there is no direct analog to tectonic uplift as the entire surface lowers during the melt season. However, it is still possible for steady state elevation profiles to form, if fluvial erosion balances radiation-driven surface melting and ice flow at all points. There are good reasons to suspect that such steady state might be rare for supraglacial streams. Ice speeds vary considerably throughout the ablation zone (0.1 – 0.4 m/d in our study area) [*Joughin et al.*, 2010b]. Rapid advection of ice over a rough bed would work against the establishment of long-lived or equilibrium channels. However, vertical thermal erosion by streams is also rapid. Measured supraglacial stream incision rates are 0.1 – 0.2 m/d or greater [*Marston*, 1983; *Isenko and Mavlyudov*, 2002], although erosion relative to background lowering of the ice surface (which is the source of meltwater) is not well constrained. We suggest that the prevalence of concave up channels with power law slope-area scaling reflects fluvial adjustment toward an erosional steady state.

Steady state longitudinal profile of streams in this environment will of course differ from rivers in which vertical motion of the substrate is the primary source of uplift. Supraglacial streams must contend with a complex ice deformation field and substantial contributions from rough bedrock. The latter influence may be accounted for if bed topography is known, so we focus on the interaction between ice flow and vertical incision of streams to predict equilibrium profiles over a flat bed.

Incision of supraglacial streams into ice occurs via thermal erosion driven by solar radiation that drives melting in excess of lowering surrounding ice (lower albedo of water versus ice), aided by frictional dissipation of heat by flowing water. Stream channels only exist if they erode more rapidly than their surroundings.

We assume steady, uniform streamflow here, neglecting contributions to the energy budget from channel curvature (meandering) [*Karlstrom et al.*, 2013] and conduction of heat into underlying ice. The vertical thermal erosion rate $\dot{b}$ in a channel is then

$$\dot{b} = -\frac{\Gamma + \tau_{\text{stream}} V}{\rho \mathcal{L}}, \tag{1}$$

where Γ parameterizes the energy balance at the air-water interface (units of W/m^2). It is assumed spatially uniform here, although this is probably not true over our Greenland transect since melt rate depends on elevation. ρ is ice density and $\mathcal{L}$ is the latent heat of fusion. The second term in equation (1) is depth-averaged viscous dissipation of heat [*Parker*, 1975], with V the average water velocity, $\tau_{\text{stream}} = \rho g h S$ the shear stress exerted on the stream bed, h the water depth, g gravity, and $S = \partial Z / \partial x$ the surface slope (assuming that Z is an increasing function of x). Substrate melting in this model increases steadily with flow rate, as in a "detachment-limited" erosional regime from terrestrial settings [e.g., *Seidl and Dietrich*, 1992]. In many ways, supraglacial streams are an ideal setting to test detachment-limited incision, as erosion thresholds common to sediment-dominated systems [*Lague et al.*, 2003] are not present.

Available field data, although still sparse, suggest that supraglacial streams exhibit power law scaling relations between discharge, channel geometry, and drainage area, similar to terrestrial fluvial settings [e.g., *Marston*, 1983; *Smith et al.*, 2015]. We use such scaling to relate local melt rate to upstream drainage area and derive a stream power law [e.g., *Seidl and Dietrich*, 1992; *Whipple and Tucker*, 1999] for supraglacial fluvial erosion,

$$\dot{b} = -\frac{\Gamma}{\rho \mathcal{L}} - K x^d \frac{\partial Z}{\partial x}. \tag{2}$$

Constant K (which depends on Γ) and exponent d derive from hydraulic scaling and are discussed further in the supporting information.

To account for dynamic topography from ice flow, we use a depth-averaged and linearized flow model developed to study the response of glaciers and ice sheets to environmental perturbations [e.g., *Nye*, 1960, 1963]. We assume that supraglacial streamflow is parallel to underlying ice velocity, restricting our attention to points lying within a stream channel. In the case of a flat bed (easily generalized to a rough bed) [*Cuffey and Paterson*, 2010], we derive a dimensionless evolution equation for topographic elevation (details in supporting information)

$$\left(\frac{\partial Z}{\partial t} + 1\right) = \mathcal{N} Z - \mathcal{R} x^d \frac{\partial Z}{\partial x} - \mathcal{A} \frac{\partial Z}{\partial x} + \mathcal{D} \frac{\partial^2 Z}{\partial x^2}. \tag{3}$$

Here Z, x, and t are (dimensionless) elevation of the stream channel, distance upstream, and time, respectively. The coefficients $\mathcal{N}$, $\mathcal{R}$, $\mathcal{A}$, and $\mathcal{D}$ involve relating depth-averaged glacier discharge $q = UH$ to gradients in local ice thickness H, depth-averaged and longitudinally averaged ice velocity U and surface slope, evaluated at steady state prior to perturbations. These coefficients, generally spatially and temporally variable, may be interpreted in terms of physical processes that control topographic evolution. They are formulated as ratios of the surface melting timescale to timescales of longitudinal compression/extension ($\mathcal{N}$, generally positive for compressive flow in the ablation zone), thermal fluvial erosion ($\mathcal{R}$), ice surface kinematic waves ($\mathcal{A}$), and ice diffusion ($\mathcal{D}$). We also use the ratio $Pe = \mathcal{R}/\mathcal{D}$, a Péclet number similar to what is found in terrestrial landscape evolution models to set the scale length of topography [*Perron et al.*, 2008a], to characterize the relative importance of fluvial erosion and ice diffusion.

Equation (3) reveals the importance of ice flow processes to supraglacial landscape evolution. Supraglacial streams occur on a range of spatial scales that are often less than the longitudinal stress coupling length ℓ, below which ice flux perturbations are balanced by longitudinal stresses rather than by flow. Topographic adjustment generally includes contributions both from Z, the local surface height, and $\overline{Z}$, the convolution of Z with a longitudinal filter [*Kamb and Echelmeyer*, 1986]. Equation (3) is derived by modeling $\overline{Z} = Z/\Phi$ where $\Phi = 1 + (\ell/L)^2$ and L is a scale length of topographic variation (details in supporting information).

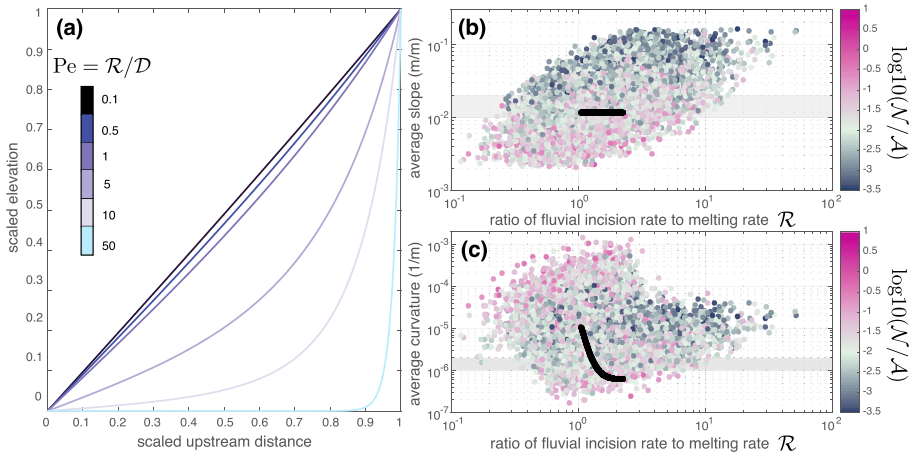

Figure 4. (a) Steady state nondimensional stream profiles from equation (3), curves vary the Péclet number $Pe = \mathcal{R}/\mathcal{D}$ that is the ratio of ice diffusion time to fluvial erosion time. (b) Monte Carlo parameter study of steady state stream profiles for uniform background ice flow over a flat bed, plotting average slope over reach length against the ratio of fluvial incision rate to melt rate $\mathcal{R}$. Black curve assumes average parameters for our Greenland study area (Table S1), varying the surface heat flux Γ. Symbols are colored by $\log10(\mathcal{N}/\mathcal{A})$, the ratio of longitudinal strain rate to ice advection rate (kinematic wave speed). The gray bar is range of values that suggest fluvial control from Figure 3. (c) Same as Figure 4b but plotting average upstream channel curvature.

Coefficients $\mathcal{N}$, $\mathcal{A}$, and $\mathcal{D}$ depend on Φ; when $L \ll \ell$ (ℓ is generally of order a few ice thicknesses) [*Kavanaugh and Cuffey*, 2009], $\Phi \to \infty$, and equation (3) simplifies to

$$\left(\frac{\partial Z}{\partial t} + 1\right) = \mathcal{N}'Z - \left(\mathcal{R}x^d + \mathcal{A}'\right)\frac{\partial Z}{\partial x}, \tag{4}$$

where $\mathcal{N}'$and$\mathcal{A}'$ are modified coefficients independent of Φ. Equation (4) demonstrates that on sufficiently small wavelengths, ice diffusion has a negligible role in surface evolution ($\mathcal{D} \to 0$), as has been previously suggested [e.g., *Gudmundsson et al.*, 1998]. Topographic adjustment then reflects a balance between melting, local longitudinal compression or extension, fluvial erosion, and advection in the background flow. Streams in our study area span a range of length scales L that sometimes exceed ℓ, so we expect that this limit holds only in the headwater regions. But longitudinal coupling probably decreases the role of ice diffusion in stream profile adjustment generally.

Steady state solutions to equation (3) are the equilibrium longitudinal profiles of supraglacial streams. Figure 4a shows the dependence of nondimensional stream profiles on fluvial incision relative to ice diffusion through *Pe*, all else fixed. When ice diffusion dominates, surface channel profiles are linear; when fluvial erosion dominates, channels are concave up. Of course, the dimensionless numbers in equation (3) covary. To assess parameter sensitivity we assume a background flow state in which basal shear stress equals the local driving stress and determine a range of values for all dimensionless coefficients that reflect general conditions in SW Greenland (discussed in the supporting information). We then conduct a Monte Carlo sweep through this parameter space, sampling a uniform prior distribution for each dimensional parameter to calculate 10,000 synthetic profiles. Figures 4b, 4c, and S6 show the results, plotting average slope and curvature over the reach length against $\mathcal{R}$, colored by $\log10(\mathcal{N}/\mathcal{A})$. Average curvature is generally the more sensitive metric: concavity of profiles increases with fluvial incision rate, longitudinal compression rate, and Φ; concavity anticorrelates with ice diffusion rate and background ice advection rate. Average slope correlates with $\mathcal{R}$ and anticorrelates with $\mathcal{N}/\mathcal{A}$. There is much scatter in these trends, but if ice flow characteristics are known a priori (black lines in Figures 4b, 4c, and S6 chosen to reflect average values from our study area), profile dependence on melt rate becomes considerably more unique.

5. Discussion

Supraglacial drainage networks exhibit planform similarities to alluvial and bedrock landscapes on similar spatial scales but erode by thermal rather than mechanical means on much more rapid timescales. Our work

suggests that, rather than being a fundamental driver of topography, fluvial control in supraglacial drainage systems is limited to spatial scales below those on which ice topography mimics bedrock roughness. Signs of stream erosion in ice sheet topography are nonetheless clear.

The combination of DEM-derived channel profiles and visual record of abandoned channels provide a record of time-evolving fluvial erosion tiled densely over the ablation zone. In combination with ice flow models [e.g., *Banwell et al.*, 2012b] that would provide the appropriate background state for channel profile analysis, analysis of stream profile evolution from DEMs made at multiple times during a melt season could constrain the interplay between ice flow and melting on $\sim 1 - 10$ km scales. We have focused on steady state profiles here, but slope transients arising from sudden changes in base level (such as lake drainage) [*Das et al.*, 2008], spatially localized ice sheet acceleration or uplift [e.g., *Ryser et al.*, 2014] may also be encoded in stream profiles, as is argued for some bedrock landscapes [e.g., *Willett et al.*, 2014].

Supraglacial channels thus potentially provide a unique probe both of underlying ice flow processes and the surface energy balance on an essentially fixed large-scale substrate. If ice velocity and bed topography are independently known, equilibrium stream concavity constrains the surface melt rate (Figure 4). Of course, steady state stream profiles in general will be more complex. The substrate upon which stream incision occurs is spatially variable due to bedrock topography, channels are not always aligned with the direction of ice flow, and ice flux will reflect spatially variable longitudinal stress coupling [*Kavanaugh and Cuffey*, 2009]. As longitudinal stress coupling dominates at small length scales, the ice is too stiff to speed up or slow down and ice flow does not strongly vary with the surface slope or ice sheet thickness (rather their spatial average). Through equation (4), fluvial erosion is balanced not by diffusion but by melting, advection in the background flow field, and longitudinal strain rate, as expressed through $\mathcal{R}$, $\mathcal{A}'$, and $\mathcal{N}'$.

We reserve a systematic deconvolution of ice flow, ice thickness and elevation, longitudinal coupling, and melt rate for future work, but note that average slopes and upstream channel curvature in our study region are consistent with observations (gray bars in Figures 4). If we take average parameters over the entire region to calculate the dimensionless coefficients (Table S1, black curves in Figures 4b and 4c), average observed curvature of $1-2\times10^{-6}$ m^{-1} implies a lowering rate of 1–4 cm day^{-1} in channels, which is similar to measured surface lowering rates of, e.g., *McGrath et al.* [2011]. For this calculation, the Péclet number $Pe \sim 1 - 10$ and $\mathcal{R} \sim 1.5$, which indicates that fluvial processes dominate both ice diffusion and background melting.

Of course, melt varies spatially, and we do see weak systematic variation of slope-area relations and stream concavity (Figures 3b and 3c) with elevation. Specifically, the lower slope and higher elevation Region 4 exhibits longer and more closely spaced streams than other study regions. Melt also varies in time [e.g., *van den Broeke et al.*, 2008]. However, it is more difficult to assess observationally whether observed streams are at equilibrium or not, as stream profiles transients are likely sensitive to the magnitude and frequency content of surface perturbations [e.g., *Royden and Perron*, 2013]. Time sequences of DEMs will provide a definitive test of longitudinal profile evolution and equilibration of channels.

It is interesting to compare signatures of supraglacial fluvial landscape evolution with other settings. As shown in Figure 3, stream longitudinal profiles at drainage areas below the range of bedrock control are generally concave up and exhibit a power law relationship between local slope and drainage area $S = k_s A^{-\theta}$, with k_s a channel steepness index and $\theta \sim 0.005$. Power law slope-area scaling in itself is not surprising and arises even in synthetic random landscapes [*Dodds and Rothman*, 1999], but the consistency of exponents for a specific range of drainage areas is suggestive of a common fluvial origin [*Whipple and Tucker*, 2002]. The exponent θ we find is however about an order of magnitude smaller than the smallest values that have been observed in terrestrial systems [e.g., *Howard and Kerby*, 1983; *Lague et al.*, 2003].

Positive slope-area scaling and negative curvature in Figure 3 at $A \leq \sim 10^5$ m^2 implies that a diffusive process dominates and smooths topography, similar to the effect of hillslope diffusion in terrestrial landscapes [*Montgomery and Dietrich*, 1992]. However, our analysis suggests that small-scale features such as 100s of meter long drainage basins and ridges may not diffuse [e.g., *Gudmundsson et al.*, 1998]. Although not modeled here, spatial variability in melting on small scales could act as the diffusive agent, enhanced in low-relief areas due to ponding of melt water and unchannelized or porous flow.

The low sensitivity of slope to drainage area is also consistent with our inference of a threshold drainage area for channelization (based on network extraction from DEMs) that is very small compared to values reported for other landscapes [e.g., *Montgomery and Foufoula-Georgiou*, 1993]. These observations suggest a supraglacial

drainage network governed by a high-supply rate and efficient channelization [*Mantelli et al.*, 2015], as also occurs in short-lived terrestrial channels [*Niemann and Hasbargen*, 2005]. Thus, for the purposes of predicting large-scale melt water routing on the Greenland Ice Sheet [e.g., *Banwell et al.*, 2012a], the overall supraglacial hydrologic flux should primarily reflect catchments set by underlying bedrock rather than transient fluvial adjustments.

Acknowledgments
L.K. acknowledges helpful discussions with Joshua Roering, Kristin Sweeney, and Brittany A. Erickson. K.Y. acknowledges support from the NASA Cryosphere Program NNX14AH93G, managed by Thomas Wagner. WorldView images and DEMs are provided by the Polar Geospatial Center, University of Minnesota. Discussion with reviewer Kurt Cuffey about the significance of longitudinal coupling effects significantly improved the model presentation. An anonymous reviewer provided additional thoughtful, constructive comments. The data used here are listed in the references, tables, and supporting information.

References

Baker, V. E., C. W. Hamilton, D. M. Burr, V. C. Gulick, G. Komatsu, W. Luo, J. W. Rice, and J. A. P. Rodriguez (2015), Fluvial geomorphology on Earth-like planetary surfaces: A review, *Geomorphology*, *245*, 149–182.

Banwell, A. F., N. S. Arnold, I. C. Willis, M. Tedesco, and A. P. Ahlstrom (2012a), Modeling supraglacial water routing and lake filling on the Greenland Ice Sheet, *J. Geophys. Res.*, *117*, F04012, doi:10.1029/2012JF002393.

Banwell, A. F., I. C. Willis, N. S. Arnold, A. Messerli, C. J. Rye, and A. P. Ahlstrom (2012b), Calibration and validation of a high resolution surface mass balance model for Paakitsoq, West Greenland, *J. Glaciol.*, *58*(212), 1047–1062.

Cuffey, K. M., and W. S. B. Paterson (2010), *The Physics of Glaciers*, 4th ed., Butterworth-Heinemann, San Francisco, Calif.

Das, S. B., I. Joughlin, M. D. Behn, I. M. Howat, M. A. King, D. Lizarralde, and M. P. Bhatia (2008), Fracture propagation to the base of the Greenland Ice Sheet during supraglacial lake drainage, *Science*, *320*(5877), 778–781.

Dodds, P. S., and D. H. Rothman (1999), Unified view of scaling laws for river networks, *Phys. Rev. E*, *59*(5), 4865–4877.

Fountain, A. G., and J. S. Walder (1998), Water flow through temperate glaciers, *Rev. Geophys.*, *36*(3), 299–328.

Gilbert, G. K. (1877), Geology of the Henry Mountains, *Tech. Rep.*, 160 pp., U.S. Geographical and Geological Survey of the Rocky Mountain Region, Washington, D. C.

Gudmundsson, G. H. (2003), Transmission of basal variability to a glacier surface, *J. Geophys. Res.*, *108*(B5), 2253, doi:10.1029/2002JB002107.

Gudmundsson, G. H., C. F. Raymond, and R. Bindschadler (1998), The origin and longevity of flow stripes on Antarctic ice streams, *Ann. Glaciol.*, *27*, 145–152.

Howard, A. D., and G. Kerby (1983), Channel changes in badlands, *Geol. Soc. Am. Bull.*, *94*, 739–752.

Isenko, E., and B. Mavlyudov (2002), On the intensity of ice melting in supraglacial and englacial channels, *Bull. Glaciol. Res.*, *19*, 93–99.

Joughin, I., B. Smith, I. Howat, and T. S. T. Moon (2010a), Greenland flow variability from ice-sheet-wide velocity mapping, *J. Glaciol.*, *56*(197), 415–430.

Joughin, I., B. Smith, I. Howat, and T. Scambos (2010b), MEaSUREs Greenland Ice Sheet velocity map from InSAR data, version 1 [collected 2011], *Tech. Rep.*, NASA National Snow and Ice Data Center Distributed Active Archive Center, Boulder, Colo. [Available at http://dx.doi.org/10.5067/MEASURES/CRYOSPHERE/nsidc-0478.001.]

Kamb, B., and A. Echelmeyer (1986), Stress-gradient coupling in glacier flow: 1. Longitudinal average of the influence of ice thickness and surface slope, *J. Glaciol.*, *32*(111), 267–284.

Karlstrom, L., P. Gajjar, and M. Manga (2013), Meander formation in supraglacial streams, *J. Geophys. Res. Earth Surf.*, *118*, 1897–1907, doi:10.1002/jgrf.20135.

Kavanaugh, J. L., and K. M. Cuffey (2009), Dynamics and mass balance of Taylor Glacier, Antarctica: 2. Force balance and longitudinal coupling, *J. Geophys. Res.*, *114*, F04011, doi:10.1029/2009JF001329.

Lague, D., A. Crave, and P. Davy (2003), Laboratory experiments simulating the geomorphic response to tectonic uplift, *J. Geophys. Res.*, *108*(B1), 2008, doi:10.1029/2002JB001785.

Lampkin, D. J., and J. VanderBerg (2011), A preliminary investigation of the influence of basal and surface topography on supraglacial lake distribution near Jakobshavn Isbrae, western Greenland, *Hydrol. Process.*, *25*(21), 3347–3355.

Liang, Y.-L., W. Colgan, Q. Lv, K. Steffen, W. Abdalati, J. Stroeve, D. Gallaher, and N. Bayou (2012), A decadel investigation of supraglacial lakes in West Greenland using a fully automatic detection and tracking algorithm, *Remote Sens. Environ.*, *123*, 127–138.

Mantelli, E., C. Camporeale, and L. Ridolfi (2015), Supraglacial channel inception: Modeling and processes, *Water Resour. Res.*, *51*, 7044–7063, doi:10.1002/2015WR017075.

Marston, R. A. (1983), Supraglacial stream dynamics on the Juneau Icefield, *Ann. Assoc. Am. Geogr.*, *73*(4), 597–608.

McGrath, D., W. Colgan, K. Steffen, P. Lauffenburger, and J. Balog (2011), Assessing the summer water budget of a moulin basin in the Sermeq Avannarleq ablation region, Greenland Ice Sheet, *J. Glaciol.*, *57*(205), 954–964.

Montgomery, D. R. (2001), Slope distributions, threshold hillslopes, and steady-state topography, *Am. J. Sci.*, *301*, 432–454.

Montgomery, D. R., and W. E. Dietrich (1992), Channel initiation and the problem of landscape scale, *Science*, *255*, 826–830.

Montgomery, D. R., and E. Foufoula-Georgiou (1993), Channel network source representation using digital elevation models, *Water Resour. Res.*, *29*(12), 3925–3934.

Morlighem, M., E. Rignot, J. Mouginot, X. Wu, H. Seroussi, E. Larour, and J. Paden (2013), High-resolution bed topography mapping of Russel Glacier, Greenland, inferred from Operation IceBridge data, *J. Glaciol.*, *59*(218), 1015–1023.

Müller, F., and A. Iken (1973), Velocity fluctuations and water regime of arctic valley glaciers, *Int. Assoc. Sci. Hydrol.*, *95*, 165–182.

Nagler, T., H. Rott, M. Hetzenecker, J. Wuite, and P. Potin (2015), The Sentinel-1 mission: New opportunities for ice sheet observations, *Remote Sens.*, *7*, 9371–9389.

Niemann, J. D., and L. E. Hasbargen (2005), A comparison of experimental and natural drainage basin morphology across a range of scales, *J. Geophys. Res.*, *110*, F04017, doi:10.1029/2004JF000204.

Noh, M. J., and I. M. Howat (2015), Automated stereo-photogrammetric DEM generation at high latitudes: Surface extraction with TIN-based Search-space Minimization (SETSM) validation and demonstration over glaciated regions, *GISci. Remote Sens.*, *52*(2), 198–217.

Nye, J. F. (1960), The response of glaciers and ice-sheets to seasonal and climatic changes, *Proc. R. Soc. A*, *256*(1287), 559–584.

Nye, J. F. (1963), The response of a glacier to changes in the rate of nourishment and wastage, *Proc. R. Soc. A*, *275*(1360), 87–112.

Parker, G. (1975), Meandering of supraglacial melt streams, *Water Resour. Res.*, *11*(4), 551–552.

Perron, J. T., W. E. Dietrich, and J. W. Kirchner (2008a), Controls on the spacing of first-order valleys, *J. Geophys. Res.*, *113*, F04016, doi:10.1029/2007JF000977.

Perron, J. T., J. W. Kirchner, and W. E. Dietrich (2008b), Spectral signatures of characteristic spatial scales and nonfractal structure in landscapes, *J. Geophys. Res.*, *113*, F04003, doi:10.1029/2007JF000866.

Poinar, K., I. Joughin, S. B. Das, M. D. Behn, J. T. M. Lenaerts, and M. R. van den Broeke (2015), Limits to future expansion of surface-melt-enhanced ice flow into the interior of western Greenland, *Geophys. Res. Lett.*, *42*, 1800–1807, doi:10.1002/2015GL063192.

Raymond, M., and G. H. Gudmundsson (2009), Estimating basal properties of ice streams from surface measurements: A non-linear Bayesian inverse approach applied to synthetic data, *Cryosphere*, *3*, 265–278.

Rippin, D. A., A. Pomfret, and N. King (2015), High resolution mapping of supra-glacial drainage pathways reveals link between micro-channel drainage density, surface roughness and surface reflectance, *Earth Surf. Process. Landforms*, *40*(10), 1279–1290.
Royden, L., and J. T. Perron (2013), Solutions of the stream power equation and application to the evolution of river longitudinal profiles, *J. Geophys. Res. Earth Surf.*, *118*, 497–518, doi:10.1002/jgrf.20031.
Ryser, C., M. P. Lüthi, L. C. Andrews, G. A. Catania, M. Funk, and R. Hawley (2014), Caterpillar-like ice motion in the ablation zone of the Greenland Ice Sheet, *J. Geophys. Res. Earth Surf.*, *119*, 2258–2271, doi:10.1002/2013JF003067.
Seidl, M. A., and W. E. Dietrich (1992), The problem of channel erosion into bedrock, *Catena Suppl.*, *23*, 101–124.
Smith, L. C., et al. (2015), Efficient meltwater drainage through supraglacial streams and rivers on the southwest Greenland Ice Sheet, *Proc. Natl. Acad. Sci.*, *112*(4), 1001–1006.
van de Wal, R. S. W., and J. Oerlemans (1995), Response of valley glaciers to climate change and kinematic waves: A study with a numerical ice-flow model, *J. Glaciol.*, *41*(137), 142–152.
van den Broeke, M., P. Smeets, J. Ettema, C. van der Veen, R. van de Wal, and J. Oerlemans (2008), Partitioning of melt energy and meltwater fluxes in the ablation zone of the west Greenland Ice Sheet, *Cryosphere*, *2*, 179–189.
Whipple, K. X., and G. E. Tucker (1999), Dynamics of the stream-power river incision model: Implications for height limits of mountain ranges, landscape response timescales, and research needs, *J. Geophys. Res.*, *104*(B8), 17,661–17,674.
Whipple, K. X., and G. E. Tucker (2002), Implication of sediment-flux-dependent river incision models for landscape evolution, *J. Geophys. Res.*, *107*(B2), doi:10.1029/2000JB000044.
Willett, S. D., S. W. McCoy, J. T. Perron, L. Goren, and C.-Y. Chen (2014), Dynamic reorganization of river basins, *Science*, *343*(6175), 1248765.
Yang, K., L. C. Smith, V. W. Chu, C. J. Gleason, and M. Li (2015), A caution on surface use of surface digital elevation models to simulate supraglacial hydrology of the Greenland Ice Sheet, *IEEE J. Sel. Top. Appl. Earth Observ. Remote Sens.*, *8*(11), 5212–5224.